# Accepted Manuscript

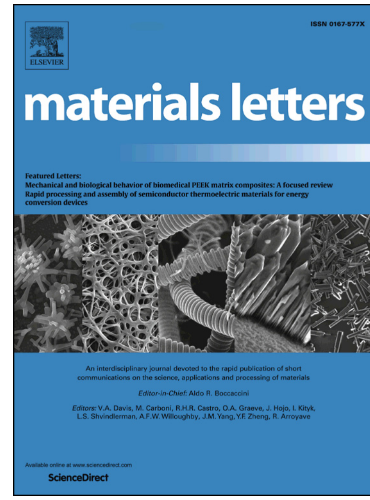


Influence of grain boundary misorientations on the mechanical behavior of a near-α Ti-6Al-7Nb alloy processed by ECAP

V.V. Polyakova, I.P. Semenova, A.V. Polyakov, D.K. Magomedova, Y. Huang, T.G. Langdon

PII: S0167-577X(16)31967-X
DOI: http://dx.doi.org/10.1016/j.matlet.2016.12.083
Reference: MLBLUE 21895

To appear in: *Materials Letters*

Received Date: 11 November 2016
Revised Date: 23 December 2016
Accepted Date: 27 December 2016

# Influence of grain boundary misorientations on the mechanical behavior of a near-α Ti-6Al-7Nb alloy processed by ECAP

V.V. Polyakova[a], I.P. Semenova[ab], A.V. Polyakov [ab*], D.K. Magomedova[b], Y. Huang[c], T.G. Langdon[c]

[a] *Ufa State Aviation Technical University, 12 K.Marx street, 450008, Ufa, Russia*

[b] *Saint Petersburg State University, 28 Universitetsky pr., 198504, Peterhof, Saint Petersburg, Russia*

[c] *University of Southampton, Southampton, SO17 1BJ, UK*

*Corresponding author: alex-v.polyakov@mail.ru

**Abstract**

A near-α Ti-6Al-7Nb alloy was processed by equal-channel angular pressing (ECAP) and the features of microstructural transformation were studied using EBSD analysis and transmission electron microscopy. The results show a non-monotonic variation in the density of low-angle and high-angle boundaries of the α-phase grains with increasing strain during ECAP. The relationship between the misorientations of the grain boundaries and the mechanical properties of the alloy were examined.

**Keywords**: titanium alloy; ultrafine-grained structure; grain boundaries; strength; ductility.

## Introduction

The Ti-6Al-7Nb alloy was designed especially for medical applications as a more inert analogue of the Ti-6Al-4V alloy [1]. However, unlike the Ti-6Al-4V, the Ti-6Al-7Nb alloy is practically not hardened by conventional heat treatment (HT), since it belongs to the near-α Ti alloys in which the content of the β-phase is not more than 5% [2]. As is well known, severe plastic deformation (SPD) techniques enable the fabrication of bulk nanostructured billets having ultrafine-grained (UFG) structures with grain sizes below 1 μm and excellent mechanical properties [3]. An enhancement in the strength of the Ti-6Al-7Nb alloy due to UFG structure formation will enable, in many cases, a successful replacement of Ti-6Al-4V and stainless steels which are traditionally used in osteosynthesis and orthopedics.

In practice, the grain boundaries (GB) in UFG materials play a key role in their mechanical behavior [4] and there is a possibility of controling the mechanical behavior through the use of grain boundary engineering [5]. The UFG structure formation in metals under SPD depends on the processing regimes, which leads to establishing various types of boundaries such as high-angle, low-angle, special and random, equilibrium and non-equilibrium boundaries [4,5].

The aim of the investigation was to study the deformation mechanisms of the formation of new intergranular and inter-phase boundaries and to reveal the relationship between the microstructural evolution and the mechanical properties of the Ti-6Al-7Nb alloy.

## Experimental methods

The Ti-6Al-7Nb (IMI 367) rods in a diameter of 22 mm were subjected to HT at 985°C for 1h, quenched, then annealed at 750°C for 4h for the formation of a duplex (equiaxed-lamellar) structure. The ECAP was conducted at 600°C using Bc route in a die-set with a channel intersection angle of 120°. The numbers of ECAP passes ($n$) were from 1 to 6 and, according to the equation $\varepsilon_n = \frac{2}{\sqrt{3}} ctg \frac{\varphi}{2}$ [6], the strain ($\varepsilon$) for 1 pass is 0.67.

A study of GB misorientations was conducted by automatic analysis of electron backscattered diffraction (EBSD) obtained using a scanning electron microscope Philips XL40 FESEM with field emission and TSL OIM 6 (EDAX) software. The step sizes were 200 and 30 nm. From the ratio of the total length of the low-angle boundaries (LAB <15º) and high-angle boundaries (HABs) to the scanned area, the values of the densities of boundaries were defined [7]. The microstructure was studied using a JEM 2100 electron microscope.

Tensile mechanical testing was performed at RT with a strain rate of $1\times10^{-3}$ $s^{-1}$. The specimens had cylindrical sections of 3 mm in diameter with gauge lengths of 15 mm.

**Results and discussion**

Figure 1a shows an EBSD grain map of the initial structure after HT consisting of primary α-phase grains and colonies of α-phase plates. After 2 passes ECAP in Fig. 1b, the microstructure consists of fragments of severely distorted plates which appear to be broken by LAB in addition to small globular grains of the α- and β-phases. The larger grains of the primary α-phase are characterized by a developed substructure in Fig. 1b.

Figure 2a,b shows typical TEM images of the fragmented primary α-phase at different magnifications after 2 passes of ECAP. As a result of the SPD, there is an increase in the dislocation density in the bodies of larger grains with the formation of weakly misoriented structures of a cellular type. The lamellar structure has transformed with the formation of subgrain boundaries with a high dislocation density.

After reaching strain 2.68 and 4.02, the structure forms a GB ensemble from fully spheroidized grains/subgrains of the α- and β-phases where two types of grains can be noted: new grains with equilibrium boundaries and those with non-equilibrium boundaries of deformation origin (Fig. 3a). The average sizes of the α- and β-phases grains/subgrains after 4 and 6 passes are similar and reached values of 350 and 330 nm, respectively (Fig. 3b). Fig. 3c shows the distribution of the β-phase in the EBSD phase contrast map after 6 passes of ECAP. The β-phase (bright contrast) is distributed in the form of separate grains with sizes from 300 to 500 nm and therefore it has approximately the same size as the α-phase grains.

Using the EBSD analysis, the dependencies the LABs and HABs densities ($\rho_B$) on strain of ECAP are shown in Fig. 4a. It can be seen that in the initial state the density of LABs is on average to 0.15±0.04 $\mu m^{-1}$ whereas the density of HABs is 1.2±0.3 $\mu m^{-1}$. With an increase in strain from 1.34 to 4.02, the density of HABs monotonically increases, thereby indicating an increase in the length of the boundaries and the formation of smaller grains. The density of HABs at strain 4.02 was 6.5±0.8 $\mu m^{-1}$. It is important to note that, under the same strains, the fraction of LABs does not change significantly and even slightly decreases after 6 passes, amounting to 2.4±0.43 $\mu m^{-1}$. Therefore, it can be seen in Fig. 4a that the incremental rate of HABs is noticeably higher than the growth of LABs. As the accumulated strain increases, this difference becomes significant due to the predominant transformation of subgrain boundaries into HABs although the formation of new LABs also continues. The increase in the amount of HABs with increase in the dispersion degree of the structure in the Ti-6Al-7Nb facilitates the occurrence of grain boundary sliding (GBS), which eventually becomes manifest in a reduction of the plastic flow stress and thereby in an increase of the ductility as observed after 6 passes of ECAP [8].

Figure 4b shows the change in the strength and ductility of the Ti-6Al-7Nb alloy during ECAP. An increase in the dislocation density and the formation of a developed dislocation ensemble in the plates and primary α-phase grains after 2 passes is the main reason for the sharp increase in the density of LABs (Fig. 4a). This leads to a significant enhancement of the strength (1050 MPa) due to the cumulative action of the strengthening mechanisms caused by irregular dislocation tangles and the organized substructures. Such structural changes correspond to a decrease in ductility ($\delta \sim 9\%$). However, with a further increase in strain up to 4.02, the strength increases up to 1200 MPa, the ductility also grows and the elongation reaches 12% (Fig. 4b). Thus, the average size of the α-phase grains after 4 and 6 passes does not change significantly (350 and 330 nm, respectively), while the density of HABs grows visibly as in Fig. 4a. Thus, the enhancement in the strength with increasing fraction of HABs may be related to the Hall-Petch relation, since with decreasing grain size the total length of boundaries increases. At the same time, HABs promote the mechanisms of GBS and/or contribute to strain hardening during plastic deformation which leads to ductility enhancement [4,5]. LABs or subgrains make a contribution to strength due to the mechanism of dislocation hardening which is less efficient than the grain-boundary mechanism (due to HABs).

The present results show that SPD provide new opportunities for GB design through the fabrication of UFG and nanocrystalline metals and alloys [4]. Therefore, the research results obtained in this study for the Ti-6Al-7Nb alloy confirm that the structure of boundaries of new grains, formed after SPD, has a significant effect on the mechanical behavior of these UFG materials.

## Conclusions

Microstructure evolution in the Ti-6Al-7Nb alloy subjected to ECAP was studied. Fragmentation of the primary α-phase grains is realized through the slip and accumulation of dislocations with the formation of predominantly subgrain boundaries. A transformation of the initial lamellar fraction leads to the formation of high-angle boundaries. The dependence of the density of LABs and HABs on the strain has a stage character. The formation of an UFG structure in the Ti-6Al-7Nb alloy with a mean size of 330 nm leads to an increase in the UTS up to 1210 MPa, where this is 20% higher than for the hot-rolled counterpart.

## Acknowledgements

ECAP and mechanical testing was supported by the Russian Science Foundation № 16-19-10356 in «USATU», the TEM analyses – by the RFBR grant №16-58-1006116. The work of two authors was supported by the European Research Council under ERC Grant Agreement No. 267464-SPDMETALS (YH and TGL). The authors thank V.N. Anumalasetty for help with the EBSD analysis.

**References**.

[1] D.M. Brunette, P. Tengvall, M. Textor, P. Thomsen, Titanium in Medicine, Springer-Verlag Berlin Heidelberg, Germany, 2001.

[2] R. Boyer, G. Welsch, E. Collings, Materials Properties Handbook: Titanium Alloys, ASM International, Metals Park, OH, USA, 1998.

[3] R.Z. Valiev, Y. Estrin, Z. Horita, T.G. Langdon, M.J. Zehetbauer, Y.T. Zhu, Producing Bulk Ultrafine-Grained Materials by Severe Plastic Deformation, JOM 58, 4 (2006) 33–39.

[4] R.Z. Valiev, On grain boundary engineering of UFG metals and alloys for enhancing their properties, Mater Sci Forum 584-586 (2008) 22-28.

[5] I.P. Semenova, G.H. Salimgareeva, G.Da Costa, W. Lefebvre, R.Z. Valiev, Enhanced strength and ductility of ultra-fine grained Ti processed by severe plastic deformation, Adv Eng Mater 12 (2010) 803-807.

[6] V.M. Segal, Materials processing by simple shear, Mater Sci Eng. A197 (1995) 157-164.

[7] V.N Anumalasetty, G. Colombo, G. McIntosh, Yu. Mardakhayeva, D. Yu, Microstructure and mechanical properties of coarse and ultrafine grain titanium with different iron contents, In: Proceeding of PRICM-8, Wiley (2013) 3265-3273.

[8] S. Mironov, M. Murzinova, S. Zherebtsov, G.A. Salishchev, S.L. Semiatin, Microstructure evolution during warm working of Ti–6Al–4V with a colony-α microstructure, Acta Mater 57 (2009) 2470–2481.

**Figure captions**

Fig. 1 EBSD grain map of the Ti-6Al-7Nb alloy: (a) initial microstructure; (b) 2 passes ECAP.

Fig. 2 TEM images after 2 passes ECAP: (a) primary α-phase grains (region A) and deformed α- grains (region B); (b) deformed (α+β)- region.

Fig. 3 Microstructure of the Ti-6Al-7Nb alloy after 6 passes ECAP: (a) bright-field TEM image; b) EBSD grain map; c) EBSD phase contrast map (β-phase).

Fig. 4 Dependence of LABs and HABs density (a) and UTS with elongation (b) on the strain value ($\varepsilon$) of ECAP Ti-6Al-7Nb alloy.

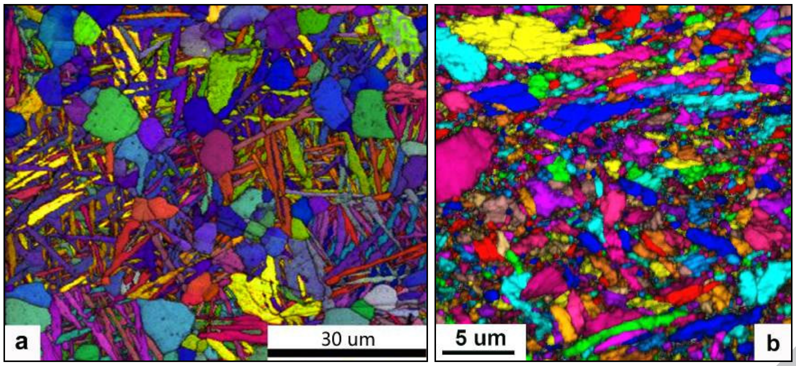


Fig. 1

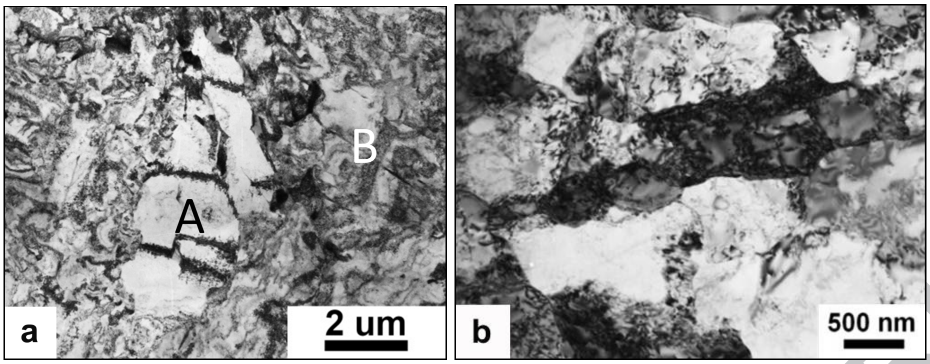


Fig. 2

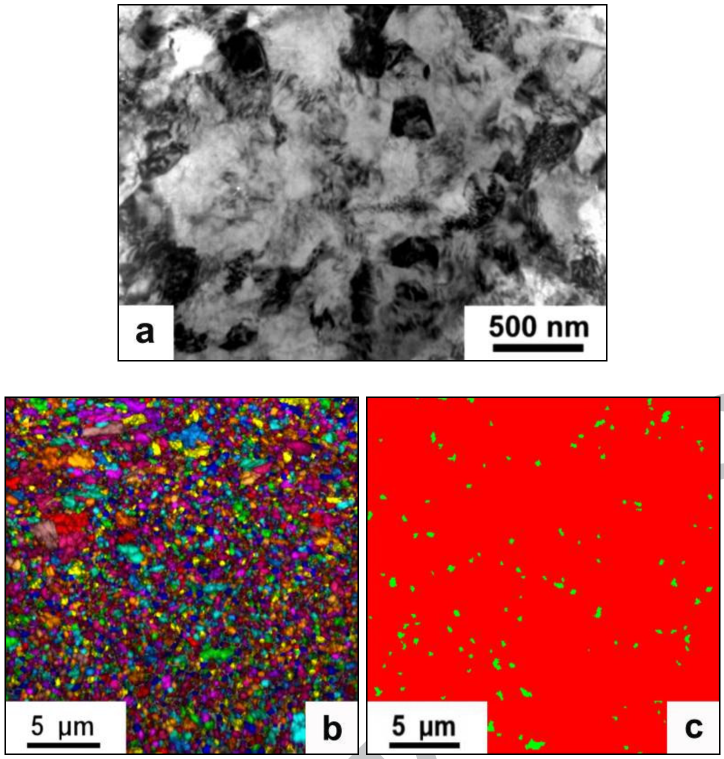


Fig. 3

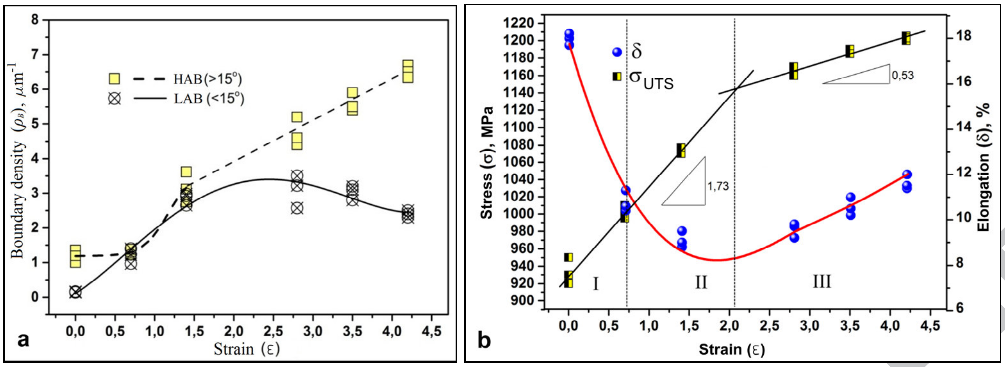
a
Boundary density ($\rho_s$), $\mu m^{-1}$
Strain (ε)
HAB(>15°)
LAB (<15°)
b
Stress (σ), MPa
Elongation (δ), %
Strain (ε)
δ
$\sigma_{UTS}$
1,73
0,53
I
II
III

Fig. 4

*Highlights (for review)

- The microstructure evolution of equiaxed and lamellar fraction of near-α Ti-6Al-7Nb alloy during the ECAP processing was studied.
- The low- and high-angle boundaries have a non-monotonic variation in density during the ECAP processing.
- An increase in the fraction of high-angle boundaries in the ultrafine-grained structure as strain reaches $\varepsilon \approx 4$ leads to an enhancement in both the strength and the ductility.